PL ISSN 0033-2097, e-ISSN 2449-9544

9'2024

PRZEGLĄD ELEKTROTECHNICZNY

ROK 100

WYDAWNICTWO SIGMA-NOT

cena 85 zł
(w tym 8% VAT)

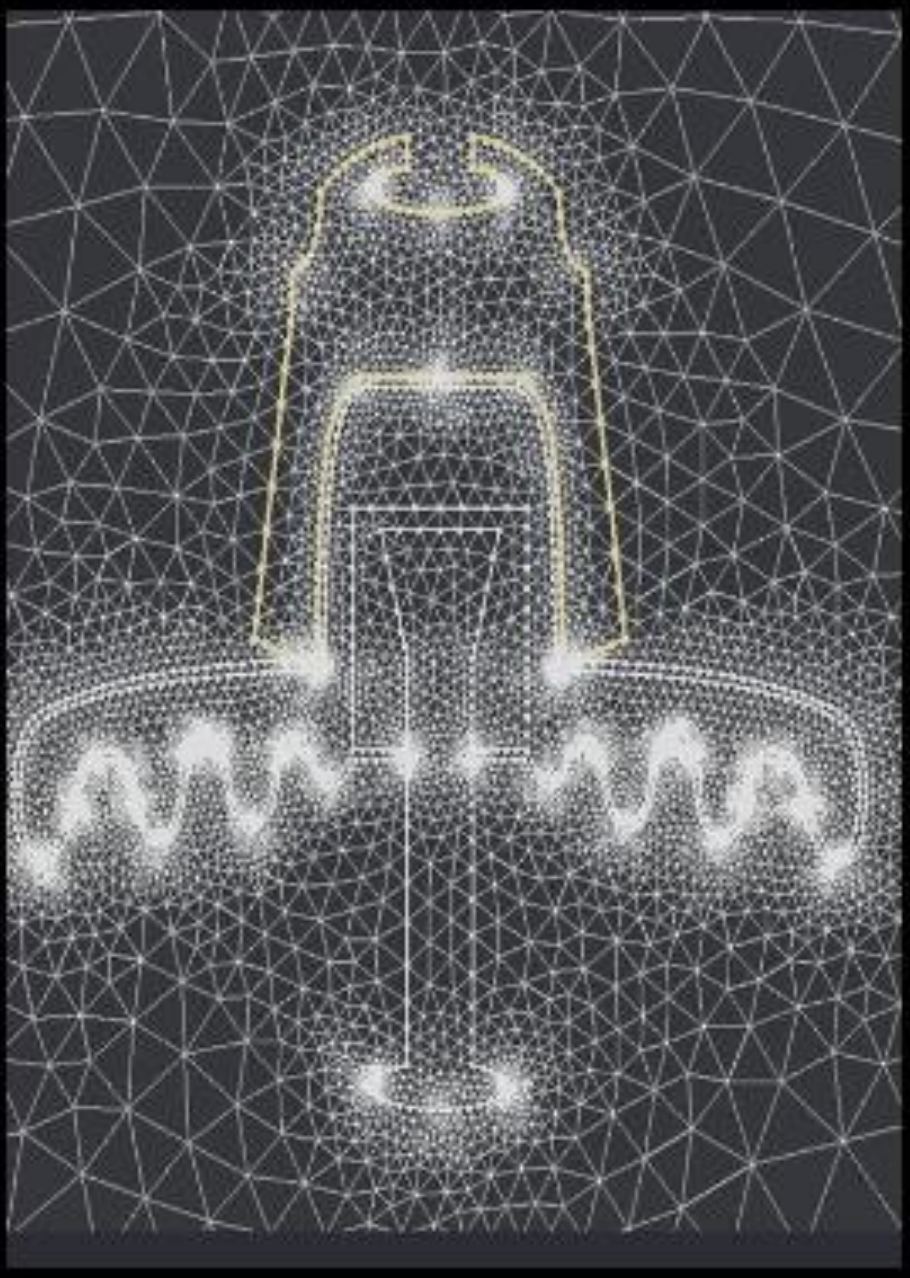

Performance Evaluation of cap and pin insulator under pollution conditions using Finite element method (FEM)
Page 142

PRZEGLĄD ELEKTROTECHNICZNY Vol 2024, Nr 9

Spis treści

PRZEGLĄD ELEKTROTECHNICZNY Vol 2024, Nr 9

Spis treści

1. Oleksandr VOZNYAK[1], 2. Yurii POLIEVODA[1], 3. Olena SOLONA[1], 4. Vitalii YAROPUD[1], 5. Ihor TVERDOKHLIB[1], 6. Mykhailo KARPIICHUK[1], 7. Kateryna KOVALOVA[1], 8. Alla SOLOMON[1]

Vinnytsia National Agrarian University (1)
ORCID: 1 0000-0002-0986-6869; 2. 0000-0002-2485-0611; 3. 0000-0002-4596-0449; 4. 0000-0003-0502-1356; 5. 0000-0003-1350-3232; 6. 0000-0003-3958-4755; 7. 0000-0001-7183-2996; 8. 0000-0003-2982-302X.

doi:10.15199/48.2024.09.11

Improvement of the electric drive of the feeder using vector PWM control

Abstract. *The article researches and develops a method of controlling an asynchronous electric motor using a microcontroller and a vector control algorithm. The use of a bidirectional timer count mode and a wide-amplitude modulation frequency allows precise adjustment of rotation speeds. The developed system is flexible due to the possibility of the external speed setting through an analog input. The application of the PI control algorithm and speed measurement sensors ensures the stability and accuracy of the system under conditions of variable loads. The results of the experiments show the high efficiency of the system with sudden changes in speed, which makes it promising for the automation of feed distribution processes. The system has a strong potential for application in the field of animal husbandry, providing an efficient and accurate control of electric motors in various operating conditions.*

Streszczenie. *W artykule zbadano i opracowano metodę sterowania asynchronicznym silnikiem elektrycznym przy użyciu mikrokontrolera i algorytmu sterowania wektorowego. Zastosowanie dwukierunkowego trybu zliczania timerów i częstotliwości modulacji o szerokiej amplitudzie pozwala na precyzyjną regulację prędkości obrotowych. Opracowany układ jest elastyczny ze względu na możliwość zewnętrznego zadawania prędkości poprzez wejście analogowe. Zastosowanie algorytmu sterowania PI i czujników pomiaru prędkości zapewnia stabilność i dokładność układu w warunkach zmiennych obciążeń. Wyniki eksperymentów pokazują wysoką sprawność układu przy nagłych zmianach prędkości, co czyni go obiecującym dla automatyzacji procesów dystrybucji pasz. Układ ma duży potencjał do zastosowania w dziedzinie hodowli zwierząt, zapewniając wydajne i dokładne sterowanie silnikami elektrycznymi w różnych warunkach pracy.*(***Udoskonalenie napędu elektrycznego podajnika z wykorzystaniem sterowania wektorowego PWM***)

Keywords: feeder, electric drive, asynchronous motor, microcontroller, vector control.
Słowa kluczowe: podajnik, napęd elektryczny, silnik asynchroniczny, mikrokontroler, sterowanie wektorowe

Introduction

The increase in production in animal husbandry is closely related to the growth in the quality of fodder and the productivity of animals, while the cost of grain for fodder is significantly reduced. One of the promising ways in animal husbandry is the use of granulated fodder and wet mixtures, which are completely balanced in terms of all necessary nutrients and elements, directly in individual feeders. In order to achieve the highest productivity with minimum consumption of the feed, highly efficient feed distribution machines are necessary. They provide accurate dosing of a given amount of feed in individual animal feeders, avoiding the losses of feed materials and providing prompt adjustment of doses in automatic mode, taking into account productivity and individual characteristics of animals.

In order to mechanize the process of delivery and distribution of dry, liquid fodder and wet mixtures, various fodder distribution machines and devices of stationary or mobile execution are used [1].

Analyzing the ways to solve the problem

Based on the analysis of literary sources and the generalization of the research in the field of feed distribution on livestock farms and complexes, it is possible to draw a conclusion about the advantages of the using of electrified feed distributors of limited mobility. This category includes bunker dispensers that are equipped with an electric drive and move along guide rails in the feed passage, such as serial models DS-5A, FS-1.5, FSP-0.8, or trestle variants, for example, TSF-1.7 (trestle serial feeder), or dispensers installed on the chassis of electric cars.

In order to preserve the environment and reduce greenhouse gas emissions, regulations are being introduced all over the world that require manufacturers of household electrical equipment and industrial enterprises to develop and produce products aimed at more efficient consumption of electricity. One proven method of achieving this goal is effective motor speed control. This is the reason for the growing interest of home appliance developers and semiconductor suppliers in creating affordable and economical adjustable actuators in the modern era [7-9].

In order to conduct the research, we will consider the electric drive of the TSF-1.7 mobile feed dispenser, which consists of three independent electric drives that require modernization of the control system.

The control station includes contact-switching devices for manual and automatic control, power circuits for electric motors and the control system, which are protected against short circuits and overloads by means of fuses.

Electric motors are protected from overheating due to overloading by means of a two-pole thermal relay from the TR series. The mobile feeder is powered by a three-phase, four-wire alternating current network, where the neutral is blindly grounded. Line voltage is 380 V, current frequency is 50 Hz [2].

The electric drives of this type of mobile feeders use three-phase asynchronous motors with a short-circuited rotor, which belong to the old series. The control scheme is implemented using relay-contact devices, the production of which was started 20-30 years ago. Therefore, there is a need to modernize the electric drive, including the use of new series of asynchronous motors and modern methods of their control [10-12, 14-17].

So, in order to understand effective motor control, it is important to study the timing diagrams of the voltages during the commutation process. Below is the expression of the electric moment, which is generated by one phase:

$$T_e = \frac{e \cdot i}{\omega}, \quad (1)$$

where T_e – is the electric moment; e – EMF; i – motor winding current; ω – is the angular speed of the rotor.

This expression indicates that the torque, which is produced, is in the same direction as the direction of motion, when the voltage (*e*) and current (*i*) have the same sign. On the other hand, if the voltage and current have

opposite signs, electrical energy is wasted in slowing down the motor.

Most motors use a rectangular voltage waveform during commutation, known as block commutation. With block commutation, the switching occurs at the crossing of the voltage of the electromagnetic force (EMF) of zero level to ensure the same sign of the phase current and the EMF.

Formation of the research objective

The goal is to modernize the electric drive of mobile feeders to improve their efficiency, accuracy and reliability in conditions of modern technologies and requirements to electromechanical

systems. The problems mentioned in the work require improvement and the aim of modernization is to

solve these problems with the help of new technologies and management methods.

Materials and methods

Speed control using pulse width modulation. In addition to controlling the engine speed, there may be a need to reduce acoustic noise and reduce its power consumption [5, 6].

In order to control the engine speed, one of the methods is to adjust the operating voltage. However, many systems, including PCs, cannot directly generate a regulated voltage to power an electric motor without an additional hardware power stage. This leads to the introduction of a special scheme that allows you to adjust the supply voltage, increasing the cost of the entire system. Paying attention to the fact that the drive electronics already include transistors to control the motor supply voltage, the use of an additional circuit to regulate the voltage is ineffective [7-9]. One alternative solution for voltage and speed control is to use electronics to control the motor. When using a microcontroller to control the switching, you can use pulse width modulation (PWM) to control the average voltage across the windings. The duty ratio of the PWM signal determines the average value of the voltage on the windings. Also it is shown the filling of pulses at the level of 50%. This means that the average voltage applied to the windings is 50% of the initial supply voltage. An increase in the fill factor of the PWM signal leads to an increase in the rotation speed and torque of the motor (Fig. 1).

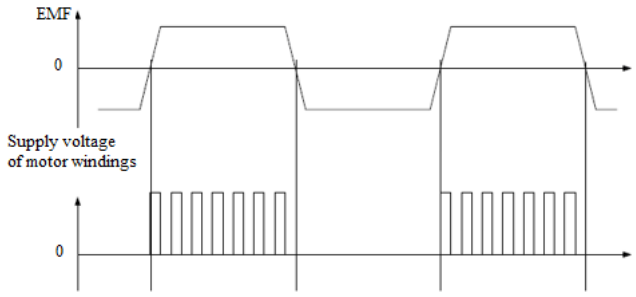

Fig. 1. Supply voltage of motor windings with PWM

When using PWM speed control, it is desirable to have a built-in hardware PWM signal generator in the microcontroller. The use of a hardware PWM generator ensures the accuracy of the timing diagram without spurious pulses, which allows you to adjust the voltage (pulse fill) over the entire range from 0% to 100%. Hardware PWM signal generation also frees up the processor for other important tasks, such as switching control, protection functions, and speed stabilization.

When using PWM speed control, it is important to place the fundamental frequency of the PWM outside the audible range, which typically ranges from 20 Hz to 20 kHz. This requires the use of a PWM fundamental frequency well above 20 kHz. At the same time, it is also necessary to take into account the mechanical characteristics of the engine. Although acoustic noise is often inaudible even when the PWM base frequency is below 20 kHz, it is important to note that as the PWM base frequency increases, the power dissipated in the control transistors increases.

The specified rotation frequency. In most cases, the engine speed can be controlled by an external signal. This signal can be analog, generated, for example, by a temperature sensor or potentiometer, or a PWM signal generated by the main controller of the system. Using a microcontroller with an integrated ADC, any type of external signal can be used to set the motor speed. After determining the set speed, it is possible to change the filling of pulses of the PWM signal to control the supply voltage of the windings. Thus, it is possible to implement a feedback control system where the PWM signal is constantly changing to minimize the difference between the set and actual speed.

Fig. 2 presents the main hardware functional units necessary to create a sensor-free motor control system based on a microcontroller. The node labeled "Control Circuit" usually includes two switches that, when turned on, allow electrical current to flow through the windings. Transistors are used as keys. Capacitors located in parallel with transistors serve to smooth transient voltages that occur when the inductive load is switched off, as well as to reduce noises that occur during switching [3].

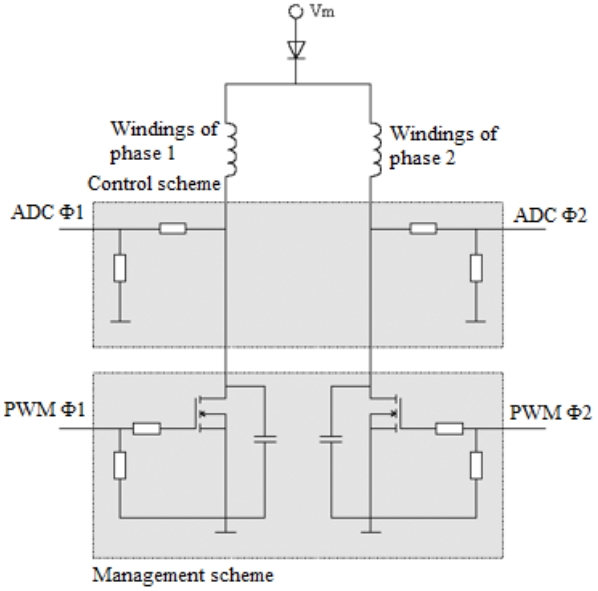

Fig. 2. Drivers and control scheme at engine management without sensors

The node labeled "Control Circuit" is responsible for signal processing. In Figure 2, only a voltage divider is used for this, which allows you to match the voltage of the signal source from the analog-to-digital converter (ADC) of the microcontroller. Without using a voltage divider, the measured voltage will be:

$$V_m - V_d - V_c, \quad (2)$$

where V_d – is the voltage drop across the diode, and V_c – is the total voltage drop across the winding.

The voltage drop across the winding is equal to the EMF of the inactive winding. Measurement of negative EMF levels is possible thanks to the location of EMF measurement points and resistive measuring circuits. In this case, negative EMF levels are superimposed on a positive constant bias. The diode, located between the supply

voltage and the motor windings, performs the function of protection against polarity reversal and ensures that the voltage from the motor does not enter the power circuit. Conclusions labeled "ADC F1/2" and "PWM F1/2" are connections to the microcontroller.

Sensorless motor control requires two ADC channels for EMF measurement and two PWM outputs for commutation and speed control. In addition, one ADC channel may be required for an external speed reference. An additional output may be required if rotation power should be measured. So, in total six lines of input and output (I/O) are required.

Fig. 3 shows the distribution of the microcontroller pins. It is important to note that the signal with information about the rotation frequency is generated at the reset pin. The RSTDISBL (reset disable) configuration bit should be programmed to enable the reset pin to operate as an I/O line. It should also be noted that even if the RSTDISBL bit is programmable, the microcontroller can be reset if a voltage higher than 10.5 V is applied to the reset input. If this feature is going to be used (i.e. a high voltage can be applied to the reset pin), a voltage limiter to the V_{cc}, level, such as a zener diode, should be provided in the the signal circuit associated with the reset pin. If necessary, it is possible to switch the output of the measured speed signal and the external speed reference.

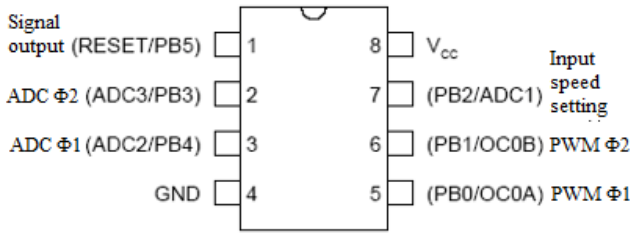

Fig. 3. Connection to the microcontroller

When measuring with an ADC, an internal reference voltage source of 1.1 V is used. Thus, all signals at the input of the ADC must vary within 0-1.1 V.

Two PWM channels are used to control the voltage of the active winding and, accordingly, the speed of rotation of the motor. The output data of these channels are connected to the transistors of the control stage. A bidirectional timer-counter is used to implement PWM. The timer generates three events: two – match events that set or clear the corresponding output, and one – which interrupt on overflow. The diagram of the bidirectional counting mode and PWM output is shown in Fig. 4.

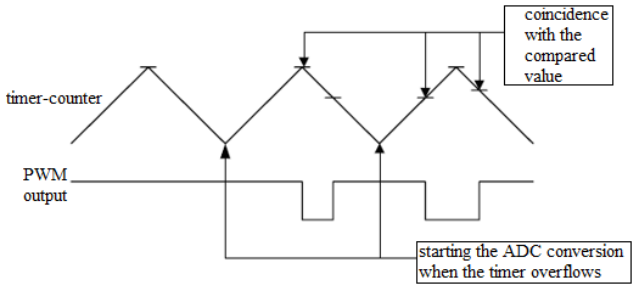

Fig. 4. PWM output of the timer-counter in bidirectional counting mode

The use of the bidirectional timer counting mode is due to the possibility of starting the ADC conversion when the timer overflows, when switching noises do not affect the EMF signal. When an interrupt occurs after the timer overflows, an interrupt handling procedure is performed in which the rotor position is evaluated and, under appropriate conditions (for example, when the EMF measured by the ADC crosses a set threshold), switching is performed.

In order to keep the PWM base frequency out of sensitivity, use a value of 240 for the top of the timer digit, which works in bidirectional regime from the internal 9.6 MHz RC oscillator. This gives a PWM frequency of about 20 kHz (9.6 MHz / 20 kHz / 2). If the frequency of the internal RC oscillator is increased by 10%, this will also increase the base frequency of the PWM without adversely affecting the operation of the microcontroller.

Preliminary positioning of the rotor is performed by increasing the supply voltage of the windings and delaying for a given time until the moment when the rotor is set in the desired position. After that, the supply voltage of the windings is reduced so that the rotor goes to rest. The initial start of the motor is without feedback, and the intervals between the switches are determined by the conversion scheme. This approach allows you to adapt the control to the mechanical characteristics of a specific engine.

Delays between switching windings can be calculated, taking into account the known acceleration characteristics of the motor. Another option is to determine the engine acceleration time by monitoring the voltage on the windings using an oscilloscope.

After the start-up sequence is complete, commutation occurs without the use of position sensors, activating an interrupt when the timer counter overflows. A block switching scheme is used, where a built-in ADC is used to measure EMF. The value of the measured EMF is compared with the limit value and if the EMF crosses this threshold, the windings are switched. To avoid errors that may occur due to transients during switching, the last few measurements are ignored.

Input of the set speed is done through an analog input, which the microcontroller converts into a digital signal to determine the desired motor speed. The reading of the specified rotation frequency occurs in the timer-counter interrupt processing procedure after the back EMF measurement is completed. The speed stabilization contour is implemented in the main cycle. Stabilization of the rotation frequency is carried out using the algorithm of stepwise increase/decrease of speed.

Using an open-collector output to generate a frequency-aware signal to the CPU or other device avoids the use of external components and lowers overall system cost. The software implementation of this engine control device is shown in the form of a block diagram in Fig. 5.

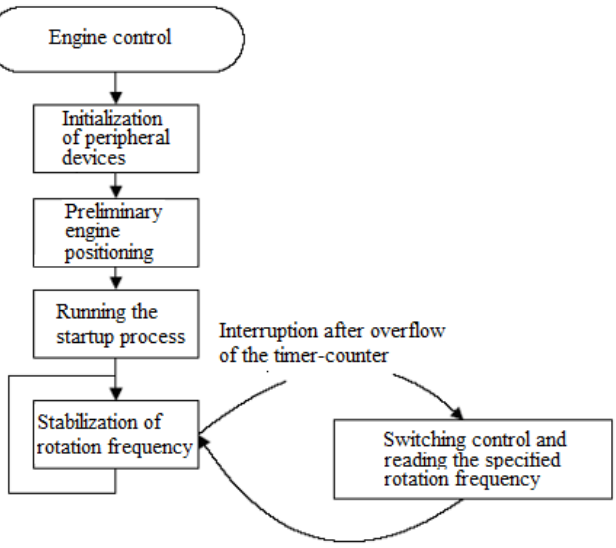

Fig. 5. Block diagram of the control program of the engine

However, the disadvantage of asynchronous motors is that they work only at nominal speed when connected to the network. This is the reason why frequency converters are necessary to regulate the frequency of rotation of asynchronous electric motors (Fig. 6). The principle of constancy of the voltage/frequency ratio is indeed widespread in modern adjustable asynchronous drives. It is ideal for applications that do not require high dynamic performance, but only require efficient speed variation over the full range.

This principle allows you to use a sinusoidal constant model of an asynchronous electric motor, where the magnitude of the stator magnetic flux is proportional to the ratio of the amplitude and frequency of the voltage of the stator winding. By keeping this ratio at a constant level, it is possible to maintain the constancy of the stator magnetic flux and, accordingly, the torque, which depends only on the slip frequency.

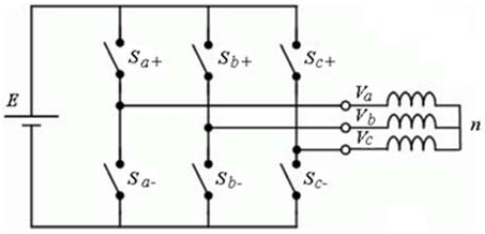

Fig. 6. Typical structure of the inverter asynchronous drive motor

Based on the usual model of an asynchronous electric motor:

$$\frac{d\phi_s}{dt} + R_s I_s = V_s; \frac{d\phi_r}{dt} - j\omega_m \phi_r + R_r L_r = 0;$$

$$\phi_s = L_s I_s + L_m L_r; \phi_r = L_r I_r + L_m I_s; \quad (3)$$

$$C_{em} = \frac{3p}{2} L_m \cdot \mathrm{Im}(I_s I_r); \Omega_m = \frac{\omega_m}{p},$$

where V_s, ϕ_s, ϕ_r, I_s, I_r – stator voltage, stator and rotor magnetic fluxes, stator and rotor currents, respectively; R_s, R_r, L_S, L_r, L_m, ω_m – total stator resistance, rotor resistance, stator inductance, rotor inductance, total leakage inductance and angular frequency, respectively.

When feeding the electric motor with a three-phase sinusoidal voltage with a frequency of ω_s the constant currents in the rotor and stator will also have a sinusoidal shape with frequency ω_s and $I_r = I_{r\max} e^{j(\omega_s t + \varphi_r)}$.

Let's convert the previous expressions to the form:

$$I_s = \frac{R_r + jL_r\omega_{slp}}{\Delta} V_s; \quad I_r = -\frac{jL_m\omega_{slp}}{\Delta} V_s; \quad \phi_r = \frac{L_m R_r}{\Delta} V_s \quad (4)$$

where $\Delta = (R_s + jL_s\omega_s)(R_r + jL_r\omega_{slp}) + L_m^2\omega_{slp}\omega_s$.

However, the amplitude value can remain constant while maintaining the constancy of the ratio $V_{sm}/|\Delta|$. At high speeds, the amplitude value of the rotor magnetic flux remains constant at a constant ratio

$$V_{sm}/\omega_s : \phi_{rm} \approx \frac{L_m R_r}{R_r L_s \omega_s} = \frac{L_m}{L_s} \cdot \frac{V_{sm}}{\omega_s}.$$

Then the torque of the electric motor is proportional to the sliding frequency: $C_{em} = \frac{3p}{2} \frac{\phi_{rm}^2}{R_r} \omega_{slp}$. These expressions show that the desired values of the torque and frequency of rotation of the electric motor can be achieved if $\omega_s = \omega_m + \frac{2C_{em}R_r}{3p\phi_{rm}^2}$. At low speeds $\phi_r \approx \frac{L_m}{R_s} V_s$.

When the stator frequency drops below a certain critical point, it is necessary to keep the voltage amplitude at a constant level in order to keep the rotor magnetic flux constant. On the contrary, if the frequency exceeds the nominal value, the voltage amplitude remains at the nominal level, taking into account the saturation of the inverter keys. In this case, the magnetic flux of the rotor becomes unstable, which leads to a decrease in the torque.

The *"V/f"* control principle uses a scalar approach, applying a three-phase sinusoidal voltage to the motor windings. The amplitude of this voltage is proportional to the frequency, except for frequencies lower than the limit value and higher than the nominal value, as shown in Fig. 7. The angle of inclination of the graphical dependence of the amplitude on the frequency, which determines the ratio of the voltage amplitude to the voltage frequency, is calculated on the basis of the nominal values of the supply voltage and the frequency of the supply network specified in the passport for the electric motor. The cutoff frequency is selected as a percentage (for example, 5%) of the nominal frequency.

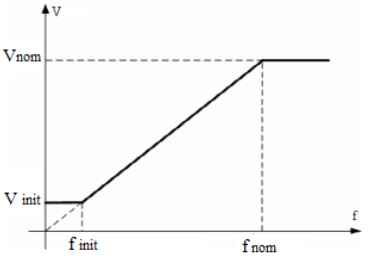

Fig. 7. Dependence of the stator voltage amplitude from the stator frequency according to the *"V/f"* principle

The *"V/f"* principle can serve as the basis for automatic speed control, as shown in Fig. 8. In this circuit, the speed deviation is compared with the desired value, and then it is given to the proportional-integral regulator (PI-regulator). The controller calculates the stator voltage frequency to provide the appropriate speed. In order to simplify the controller, the absolute value of the stator voltage frequency is used as the initial data for *"V/f"* and the vector PWM algorithm. If there is a negative value at the output of the PI controller, then the parameters controlling the power transistors of the inverter are modified to change the direction of motion of the electric motor.

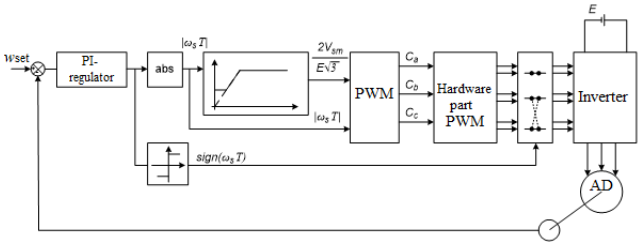

Fig. 8. Block diagram of the automatic system of speed control according to the *"V/f"* principle

Different solutions are used to determine the frequency and direction of rotation of the electric motor rotor. One of the most accurate, but also the most expensive, is the use of an absolute encoder (encoder) or an increment encoder. Optical sensors of this type have high accuracy, but also high cost, which affects the cost of the electric motor itself.

An alternative is to use a tachogenerator, which is mechanically connected to the rotor of the electric motor. This sensor requires only one analog-to-digital conversion channel to connect to the microcontroller.

The third option is the use of Hall effect sensors. These non-contact sensors have become popular due to their low cost and compact size. They include a sensor and a scheme for generating the output signal, which can be directly connected to the input-output port of the microcontroller [4].

Fig. 9 presents the transient processes for the rotation frequency and voltage of the stators obtained with the participation of the microcontroller during a jump-like change of the specified rotation speeds between +700 and -700 rpm. These results were obtained when driving an asynchronous electric motor with a power of 750 W (with a load of no more than 370 W). With the help of these graphs, it is possible to determine that the desired speed is reached within 1 second after the completion of the transient process and when the stator frequency is reached at the output of the PI controller, the value of the amplitude of the stator voltage becomes equal to the limit voltage "boost voltage".

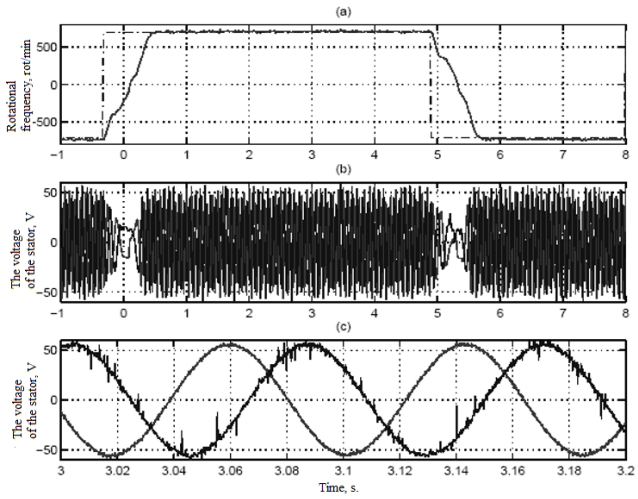

Fig. 9. Experimental results obtained using the ideal sine wave transformation table

The principle of space-vector modulation. As the electric motor is considered as a uniform load with an isolated neutral, then $V_n=(V_a+V_b+V_c)/3$; $V_{an}=V_a-V_n=(V_{ab}-V_{ca})/3$; $V_{bn}=V_b-V_n=(V_{bc}-V_{ab})/3$, but $V_{cn}=V_c-V_n=(V_{ca}-V_{bc})/3$. Paying attention to the fact that the upper power switches can only be in the on or off state, and the corresponding lower switches can only be in the opposite state (not including non-overlapping pauses in this case), eight states are possible in the power control circuit, as shown in Fig. 10. Six of them lead to the formation of non-zero phase voltages, while two alternating states lead to the formation of zero phase voltages. Applying the Concordia transformation, six non-zero phase voltages form the vertices of the hexagon (Fig. 11).

(5) $$\begin{bmatrix} V_\alpha \\ V_\beta \end{bmatrix} = \begin{bmatrix} 1 & -1/2 & -1/2 \\ 0 & \sqrt{3}/2 & -\sqrt{3}/2 \end{bmatrix}$$

As shown in Fig. 11, the angle between non-zero voltages is always 60 degrees. In complex form, these non-zero phase voltages can be written in the form $V_k=E_e^{j(k-1)n/3}$, where k = 1..6 i $V_0=V_7=0B$. The Table 1 shows the line and phase voltages for each of the eight possible configurations of the inverter.

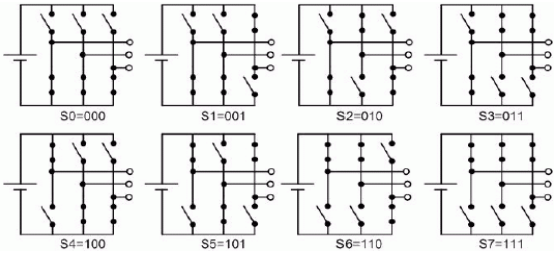

Fig. 10. Possible switching configurations of a three-phase inverter

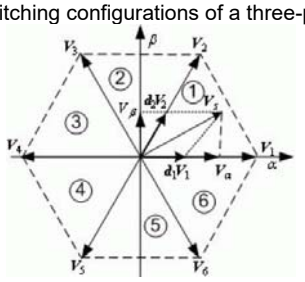

Fig. 11. Representation of eight possible inverter configurations in the system coordinates of Concordia

Table 1. States of the inverter keys and its output voltages

S_{a+}	S_{b+}	S_{c+}	S_I	V_{ab}	V_{b0}	V_{0a}	V_{an}	V_{bn}	V_{0n}	V_α	V_β	V_I
0	0	0	S_0	0	0	0	0	0	0	0	0	V_0
0	0	1	S_1	0	-E	E	$-\frac{E}{3}$	$-\frac{E}{3}$	$\frac{2E}{3}$	$-\frac{E}{2}$	$-E\frac{\sqrt{3}}{2}$	V_5
0	1	0	S_2	-E	E	0	$-\frac{E}{3}$	$\frac{2E}{3}$	$-\frac{E}{3}$	$-\frac{E}{2}$	$E\frac{\sqrt{3}}{2}$	V_3
0	1	1	S_3	-E	0	E	$-\frac{2E}{3}$	$-\frac{E}{3}$	$-\frac{E}{3}$	-E	0	V_4
1	0	0	S_4	E	0	-E	$\frac{2E}{3}$	$-\frac{E}{3}$	$-\frac{E}{3}$	E	0	V_1
1	0	1	S_5	E	-E	0	$\frac{E}{3}$	$-\frac{2E}{3}$	$\frac{E}{3}$	$\frac{E}{2}$	$-E\frac{\sqrt{3}}{2}$	V_6
1	1	0	S_6	0	E	-E	$\frac{E}{3}$	$\frac{E}{3}$	$-\frac{2E}{3}$	$\frac{E}{2}$	$E\frac{\sqrt{3}}{2}$	V_2
1	1	1	S_7	0	0	0	0	0	0	0	0	V_7

Table 2. Expressions of pulse filling factors for each sector

Number of the sector	θ	d_k	d_{k+1}
1	$\left[0,\frac{\pi}{3}\right]$	$\frac{2}{\sqrt{3}}\frac{V_s}{E}\sin\left(\frac{\pi}{3}-\theta\right)$	$\frac{2}{\sqrt{3}}\frac{V_s}{E}\sin(\theta)$
2	$\left[\frac{\pi}{3},\frac{2\pi}{3}\right]$	$\frac{2}{\sqrt{3}}\frac{V_s}{E}\sin\left(\frac{\pi}{3}+\theta\right)$	$\frac{2}{\sqrt{3}}\frac{V_s}{E}\sin\left(\frac{5\pi}{3}+\theta\right)$
3	$\left[\frac{2\pi}{3},\pi\right]$	$\frac{2}{\sqrt{3}}\frac{V_s}{E}\sin(\theta)$	$\frac{2}{\sqrt{3}}\frac{V_s}{E}\sin\left(\frac{4\pi}{3}+\theta\right)$
4	$\left[\pi,\frac{4\pi}{3}\right]$	$\frac{2}{\sqrt{3}}\frac{V_s}{E}\sin\left(\frac{5\pi}{3}+\theta\right)$	$\frac{2}{\sqrt{3}}\frac{V_s}{E}\sin(2\pi-\theta)$
5	$\left[\frac{4\pi}{3},\frac{5\pi}{3}\right]$	$\frac{2}{\sqrt{3}}\frac{V_s}{E}\sin\left(\frac{4\pi}{3}+\theta\right)$	$\frac{2}{\sqrt{3}}\frac{V_s}{E}\sin\left(\frac{2\pi}{3}+\theta\right)$
6	$\left[\frac{5\pi}{3},2\pi\right]$	$\frac{2}{\sqrt{3}}\frac{V_s}{E}\sin(2\pi-\theta)$	$\frac{2}{\sqrt{3}}\frac{V_s}{E}\sin\left(\frac{\pi}{3}+\theta\right)$

In the Concordia coordinate system, any stator voltage $V_s=V_\alpha+jV_\beta=V_{sm}cos(\theta)+jV_{sm}sin(\theta)$ falls inside one of the sectors of the hexagon and can be expressed as a linear combination of two non-zero phase voltages that define the boundaries of this sector: $V_s=d_kV_k+d_{k+1}V_{k+1}$. Equating $d_kV_k+d_{k+1}V_{k+1}$ to $V_{sm}cos(\theta)+jV_{sm}sin(\theta)$, we obtain the expressions of pulse filling coefficients for each sector, which are given in the Table 2. As the inverter cannot generate voltage V_s instantaneously, the principle of vector PWM control is to generate voltage with periodicity T_s, the average value of which is equal to V_s, which is achieved by generating voltage V_k during the period $T_k= d_k \cdot T_s$ and during the period $T_{k+1}= d_{k+1} \cdot T_s$. As $d_k+ d_{k+1} \le 1$, these voltages must be completed during the switching period T_s by the voltage V_0 and/or V_7. Several solutions are possible, in which the minimization of the total harmonic distortions of the stator

current is performed due to the application of voltages V_0 i V_7 of the same duration $T_0 = T_7 = (1 - d_k - d_{k+1})T_s/2$. The voltage V_0 is equivalent to the applied voltage at the beginning and at the end of the switching period, and V_7 is applied in the middle of the switching period. In the upper part of Fig. 12 oscillograms for sector 1 are given.

Research results

Effectiveness of implementation of vector PWM control. The Table 2 shows that the expressions for the pulse filling factors have a different form in each sector. Due to careful study of these expressions, one can come to the conclusion that since $sin(x) = sin(\pi - x)$, so all pulse filling factors can be written in a unified way: $d_k = 2V_{sm}sin(\theta'')/(E\sqrt{3})$ and $d_{k+1} = 2V_{sm}sin(\theta')/(E\sqrt{3})$, where $\theta'' = \pi/3 - \theta'$, a $\theta' = \theta - (k-1)\pi/3$. As these expressions do not depend on the sector number, they can be labeled d_a i d_b. As the range of θ' values is always within 0..π/3, when calculating d_a and d_b, a table of sines is needed only for the specified interval. This approach significantly reduces the need for memory for storing the sine table. Microcontrollers have three power cascade controllers (PSC) that generate pulse signals using a vector control algorithm [13].

The counters count from zero to a value that corresponds to a half of the switching period (as shown in the lower part of Fig. 12), and then count back to 0 again. The values to be stored in the three comparison registers are shown in Table 3.

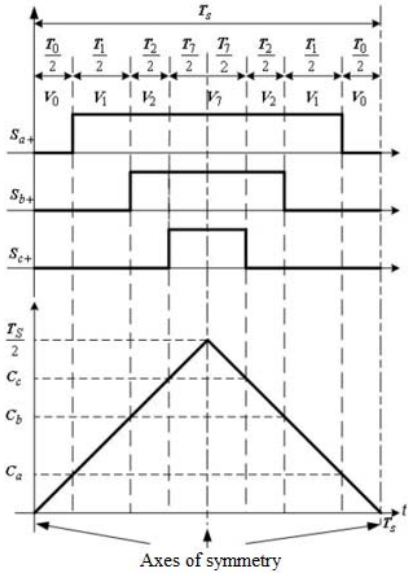

Fig. 12. Oscillograms of inventory control signals and corresponding values of comparison registers

Table 3. The value of the comparison registers depending from the sector number

The sector number	$\frac{4}{T_s}C_a - 1$	$\frac{4}{T_s}C_b - 1$	$\frac{4}{T_s}C_c - 1$
1	$-d_a - d_b$	$d_a - d_b$	$d_a + d_b$
2	$-d_a + d_b$	$-d_a - d_b$	$d_a + d_b$
3	$d_a + d_b$	$-d_a - d_b$	$d_a - d_b$
4	$d_a + d_b$	$-d_a + d_b$	$-d_a - d_b$
5	$d_a - d_b$	$d_a + d_b$	$-d_a - d_b$
6	$-d_a - d_b$	$d_a + d_b$	$-d_a + d_b$

Algorithm of the sector determination. When these values are determined by the *V/f* control principle, the moduli of the stator voltages V_{sm} are calculated by the *V/f* constancy rule, and the phase of these voltages θ is determined from ω_s using a discrete-time integrator. For effective implementation of this sector definition algorithm, it is necessary to manipulate θ' and k instead of θ in a special integrator, as shown in Fig. 13. Sector number k is the output of the counter modulo *6*, which is activated in every time θ' reaches the value of $\pi/3$. At the same time, the range of θ' values in the range $0...\pi/3$ is also limited (Fig. 14).

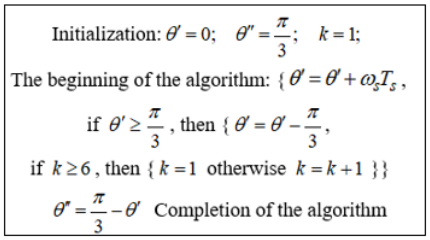

Fig. 13. Algorithm of the sector determination

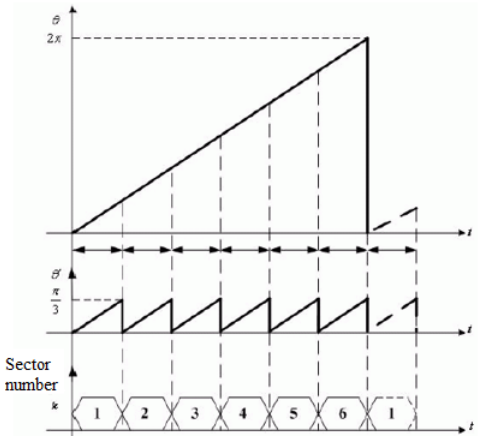

Fig. 14. Definition of the sector

Experimental verification. Fig. 15 shows the transient processes of changing the speed and voltage of the stators, obtained under the control of a microcontroller with a jump-like change of the set speed between the values of +700 and -700 rpm. These experimental results were obtained when driving a 750 W asynchronous motor (Fig. 16). From Fig. 15 it is seen that the desired speed is reached after the transient process lasting 1.2 seconds, and then, when the stator frequency at the output of the PI controller approaches zero, the stator voltage amplitude becomes equal to the threshold voltage. When using vector PWM control, the transient process is smoother (less oscillating), but longer.

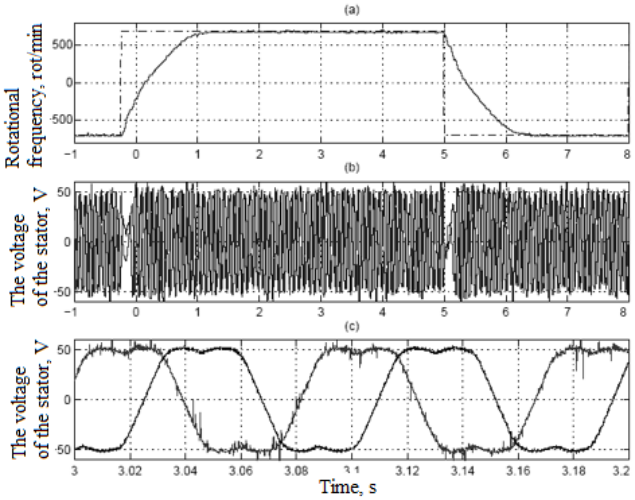

Fig. 15. Results of measurement of rotation frequency (rpm) and stator phase voltage (*V*) under microcontroller control and a jump-like change of the set rotation frequency

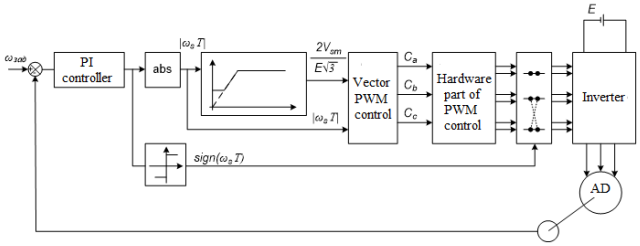

Fig. 16. Block diagram of the completed control system

Conclusions

The article investigates the modernization of an electric drive with the help of the method of controlling of an electric drive using microcontrollers and a vector control algorithm. This method is effective for regulating engine rotation in livestock and feed dispenser industries.

The system demonstrates flexibility, which makes it adaptable to different conditions and needs of the industry.

The use of the PI control algorithm and speed measurement sensors ensures the stability and accuracy of the system, especially in conditions of variable loads and different operating modes.

The results of the experiments indicate the high efficiency of the system with jump-like changes in speed, which can be a key factor in animal feeding, namely in the improvement of feeders.

Taking into account the characteristics of overclocking and transient processes when switching windings gives a powerful potential for application in the field of animal husbandry, providing efficient and accurate control of the electric motor in various operating conditions.

Funding

This research was supported and funded by the Ministry of Education and Science of Ukraine under grant № 0123U101794.

Authors: VOZNYAK Oleksandr – *PhD in Engineering, Associate Professor, Faculty of Engineering and Technology, Vinnytsia National Agrarian University (21008, 3, Sonyachna str., Vinnytsia, Ukraine, email: alex.voz1966@gmail.com);* POLIEVODA Yurii – *PhD in Engineering, Associate Professor, Faculty of Production Technology, Processing and Robotics in Livestock Husbandry, Vinnytsia National Agrarian University (21008, 3 Sonyachna str., Vinnytsia, Ukraine, e-mail: vinyura36@gmail.com);* YAROPUD Vitalii – *PhD in Engineering, Associate Professor, Dean of the Faculty of Engineering and Technology, Vinnytsia National Agrarian University (21008, 3 Sonyachna str., Vinnytsia, Ukraine, e-mail: yaropud77@gmail.com);* SOLONA Olena – *PhD in Engineering, Faculty of Production Technology, Processing and Robotics in Livestock Husbandry, Vinnytsia National Agrarian University (21008, 3, Sonyachna str., Vinnytsia, Ukraine, e-mail: solona_o_v@ukr.net);*TVERDOKHLIB Ihor – *PhD in Engineering, Associate Professor, Faculty of Production Technology, Processing and Robotics in Livestock Husbandry, Vinnytsia National Agrarian University (21008, 3 Sonyachna str., Vinnytsia, Ukraine, e-mail: igor_tverdokhlib@yahoo.com);* KARPIICHUK Mykhailo – *assistant of the Department of Electric Power Engineering, Electrical Engineering and Electromechanics, Faculty of Engineering and Technology, Vinnytsia National Agrarian University (21008, 3 Sonyachna str.,Vinnytsia,Ukraine,e-mail: mike.vnau2611@gmail.com);* KOVALOVA Kateryna – *PhD in Pedagogy, Associate Professor, Faculty of Management and Law, Vinnytsia National Agrarian University (21008, 3 Sonyachna str., Vinnytsia, Ukraine, e-mail: katrin.viter@gmail.com);* SOLOMON Alla – *PhD in Engineering, Associate Professor, Faculty of Production Technology, Processing and Robotics in Livestock Husbandry, Vinnytsia National Agrarian University (21008, 3 Sonyachna str., Vinnytsia, Ukraine, e-mail:Soloalla78@ukr.net)*.

REFERENCES

[1]. Novytskyi A.V. Reliability assessment of means for preparing and distributing fodder depending on the conditions and modes of their operation. *Scientific Bulletin of the National University of Bioresources and Nature Management of Ukraine. Series: Technology and energy of agricultural industry*. 212 (2015), nr 1, 141–148.

[2]. Velyt I.A., Korzh V.O., Pashchenko S.A. Dosers for discharge of fodder mixture of feed dispensers for pig farms. *Techniques and technologies in agro-industrial production (dedicated to the 55th anniversary of the founding of the Faculty of Engineering and Technology of the Poltava State Agrarian University): materials of the International science and practice conference*, 7-8 October, (2021), Poltava, Ukraine, 200 p.

[3]. Voytech V.O. Application of dspic33MC series Microchip microcontrollers for controlling semiconductor voltage inverters. *Proceedings of the Institute of Electrodynamics of the National Academy of Sciences of Ukraine*. 43 (2016), 107-110.

[4]. Nych O.P. Development of a synchronous electric motor control system. *Bulletin of the Khmelnytskyi National University. Technical Sciences.* 6 (2018), nr 1, 257–262.

[5]. Voznyak O.M., Shtuts A.A. Control of an AC asynchronous electric motor based on the principle of V/F constancy and conventional PWM control. *Technology, energy, transport of agricultural industry*. 119 (2022), nr 4, 102–109.

[6]. Vozniak O.M., Shtuts A.A., Tikhonov V.K. Study of starting modes of asynchronous motors and development of a soft start device. *Technology, energy, transport of agricultural industry*. 118 (2022), nr 3, 110–122.

[7]. Tsurkan O., Kupchuk I., Polievoda Y., Voznyak O., Hontaruk Y., Prysiazhniuk Y. Digital processing of one-dimensional signals based on the median filtering algorithm. *Przegląd elektrotechniczny*. 98 (2022), nr 11, 51–56.

[8]. Honcharuk I., Kupchuk I., Yaropud V., Kravets R., Burlaka S., Hraniak V., Poberezhets Ju., Rutkevych V. Mathematical modeling and creation of algorithms for analyzing the ranges of the amplitude-frequency response of a vibrating rotary crusher in the software Mathcad. *Przeglad Elektrotechniczny*. 98 (2022), nr 9, 14–20.

[9]. Spirin A.,Kupchuk I., Tverdokhlib I., Polievoda Y., Kovalova K., Dmytrenko V. Substantiation of modes of drying alfalfa pulp by activeventilation in a laboratory electric dryer. *Przegląd Elektrotechniczny* 2022. Vol. 98, № 5. P. 11-15.

[10]. Tverdokhlib I.V., Spirin A.V. Theoretical studies on the working capacity of disk devices for grinding agricultural crop seeds. *INMATEH- Agricultural Engineering*. 2016. Vol. 48, № 1. P. 43–52.

[11]. Kotov B., Spirin A., Tverdokhlib I., Polyevoda Y. Theoretical researches on cooling process regularity of the grain material in the layer. *INMATEH – Agricultural Engineering*. 54 (2018), nr 1, 87–94.

[12]. Kotov B., Spirin A., Kalinichenko R., Bandura V., Polievoda Y., Tverdokhlib I. Determination the parameters and modes of new heliocollectors constructions work for drying grain and vegetable raw material by active ventilation. *Research in Agricultural Engineering*. 65 (2019), nr 1, 20–24.

[13]. Spirin A., Kupchuk I., Tverdokhlib I., Polievoda Y., Kovalova K., Dmytrenko V. Substantiation of modes of drying alfalfa pulp by active ventilation in a laboratory electric dryer. *Przegląd Elektrotechniczny*. 98 (2022), nr 5, 11–15.

[14]. Kupchuk I., Wozniak O., Burlaka S., Polievoda Y., Vovk V., Telekalo N., Hontaruk Y. Information transfer with adaptation to the parameters of the communication channel. *Przegląd Elektrotechniczny*. 99 (2023), nr 3, 194–199.

[15]. Solona O.V., Kupchuk I.M., Derevenko I.A., Tverdokhlib I.V. Verification of the mathematical model of the energy consumption drive for vibrating disc crusher. *INMATEH – Agricultural Engineering*. 55 (2018), nr 2, 113–120.

[16]. Tsurkan O.V., Polievoda Y.A., Prysyazhnyuk D.V. et al. Vibromechanical intensification of heat and mass transfer processes during grain dehydration*: Proceedings of the International Scientific and Technical Conference*, 8-10 November, (2016), Kyiv, Ukraine, 112–114.

[17]. Solona O.V., Bilyk D.A. Vibratory mills for grinding bulk materials of agricultural production. *Vibrations in engineering and technology*. 70 (2013), nr 2, 196–199.

[18]. Tsurkan O.V., Gerasimov O.O., Polyevoda Y.A., TverdokhlibI.V., Rimar T.I., Stanislavchuk O.V. Kinetic features of vibrating and filtration dewatering of fresh peeled pumpkin. *INMATEH- Agricultural Engineering*. 2017. Vol. 52, № 2. P. 69-76.